

## LOW SPEED CARBON DEPOSITION PROCESS FOR HERMETIC OPTICAL FIBERS

**Eric A. Lindholm, Jie Li, Adam S. Hokansson, Jaroslaw Abramczyk**  
**OFS Specialty Photonics Division, Avon, CT**

**Sara E. Arthur, David R. Tallant**  
**Sandia National Laboratories, Albuquerque, NM**

### ABSTRACT

For optical fibers used in adverse environments, a carbon coating is frequently deposited on the fiber surface to prevent water and hydrogen ingress that lead respectively to strength degradation through fatigue and hydrogen-induced attenuation. The deposition of a hermetic carbon coating onto an optical fiber during the draw process holds a particular challenge when thermally-cured specialty coatings are subsequently applied because of the slower drawing rate. In this paper, we report on our efforts to improve the low-speed carbon deposition process by altering the composition and concentration of hydrocarbon precursor gases. The resulting carbon layers have been analyzed for electrical resistance, Raman spectra, coating thickness, and surface roughness, then compared to strength data and dynamic fatigue behavior.

### INTRODUCTION

In applications that demand optical fibers with high resistance to static fatigue and hydrogen-induced loss, hermetic coatings are often used. Although organic polymeric coatings are usually applied to glass fibers to provide initial

protection, these coatings cannot adequately prevent the diffusion of water or hydroxyl ions that lead to mechanical degradation. This is especially true in applications where the fiber is subjected to high temperatures and high pressures as in a geophysical or geothermal environment. For these applications, the primary function of the hermetic coating is to block water from reaching the silica glass surface to prevent the growth of microcracks and insure long-term reliability. Research into hermetic coatings are split into two areas: metallic coatings and inorganic coatings.

Metallic coatings were first investigated to improve the static fatigue resistance of optical fibers (Pinnow, et al., 1979). Although methods for coating optical fibers with metal include sputtering, vapor deposition and dip coating, the only technique known to produce hermetic metal coatings is known as "freezing", i.e. drawing the fiber through a metal melt.<sup>1</sup> Some of the metals tested have been aluminum, tin, zinc, indium, silver and gold; as such, fibers coated with metallic coatings tend to be very expensive. In addition, the freeze-coat technique is reportedly difficult to control and not well understood.<sup>2</sup> The relatively thick coatings ( $\approx 20\text{nm}$ )<sup>3</sup> can lead to unacceptable microbending losses

and long lengths of pinhole-free fiber have proven elusive.<sup>4</sup>

Inorganic coatings are applied to the glass fiber during the draw process by means of chemical vapor deposition. For carbon coatings specifically, a hydrocarbon precursor gas is introduced to the fiber at an elevated temperature ( $\approx 800$ - $1000^\circ\text{C}$ ) and thermal decomposition (a.k.a. "cracking") of the gas leads to the deposition of carbon on the surface of the glass. The applied carbon layer is typically thin ( $<100$  nm), opaque, electrically conductive, highly adherent to the glass surface via chemical bonding, and amorphous to X-ray diffraction.<sup>5</sup> Ultimately, the reactor design, the precursor gas, and the reaction temperature, will have a strong influence on the deposition rate and the characteristics of the carbon layer.<sup>6</sup>

It is well-established that the retained heat of the fiber drives the pyrolysis of the hydrocarbon to produce the bonded carbon layer. Thus, carbon deposition is largely dictated by the position of the reactor and the draw speed, which determines the fiber temperature at the reactor. Huff, et. al., further maintain that a higher fiber temperature increases the number of broken Si-O bonds on the surface of the glass which augments the Si-C chemical bonding at the glass/carbon interface.<sup>7</sup> Two corollaries that follow are that the fiber reactivity and thus the carbon deposition will be enhanced with 1.) higher draw speeds or 2.) application of the carbon coating as close to the neckdown area as possible. Moving the reactor closer to the pulling furnace has the added advantage of minimizing exposure to atmospheric water that may attach to the glass surface before the carbon layer is applied. High draw speeds ( $>5\text{m/sec}$ ) are typical when drawing

standard telecommunication fibers with UV-curable coatings. The retained heat of the fiber will be sufficient to crack the hydrocarbon in a reactor below the pulling furnace; indeed, on most high-speed towers, cooling tubes are employed to reduce the fiber temperature before the liquid coating is applied. However, the carbon deposition process takes on a special challenge when fiber is made at relatively low draw rates. This may be necessary when working with thermally-cured coatings that require a longer time to solidify on the fiber. Another limiting factor may be the in-line addition of plastic buffers (e.g. Tefzel) applied with extrusion equipment.

Because the amorphous carbon layer is conductive, the applied carbon thickness can be estimated through electrical resistance measurements. The formula<sup>8</sup> relating the resistance to thickness is:

$$R = \frac{\rho}{\pi \cdot D \cdot T}$$

- where: R = Electrical resistance ( $\text{k}\Omega/\text{cm}$ )  
 $\rho$  = Carbon layer resistance ( $\Omega \cdot \text{cm}$ )  
D = Fiber diameter ( $\mu\text{m}$ )  
T = Carbon layer thickness ( $\text{\AA}$ )

As the electrical resistance of the carbon layer decreases, either the applied carbon resistance is decreasing or the layer thickness is increasing; either of these characteristics is desirable for the purposes of improving the static fatigue performance and hydrogen-loss prevention of the fiber. Nakamura, et. al., analyzed carbon through electron spin resonance and found that lower permeability of

hydrogen correlates to an increased particle size which is further related to the extent of graphite-like carbon in the deposited layer.<sup>9</sup> Similarly, Sikora, et. al., stated that the electrical resistance is a function of crystalline size, orientation and perfection. The larger the crystalline size, the smaller the energy gap between the valence and conduction bands, thus a lower resistivity.<sup>10</sup>

Table 1: Electrical resistance of carbon

	Carbon layer resistance
Amorphous carbon	$60 \times 10^{-4} \Omega \bullet \text{cm}$
Graphite crystal	$0.39 \times 10^{-4} \Omega \bullet \text{cm}$
Calculated <sup>11</sup> resistance of 300Å thick carbon layer on 125µm fiber at 15 kΩ/cm	$17.6 \times 10^{-4} \Omega \bullet \text{cm}$

Assuming a constant resistivity, a lower electrical resistance would indicate a thicker applied layer. The accepted model for the applied carbon is that of disordered platelets (sometimes called "ribbons"), or small graphitic crystals, attaching to the glass surface and forming a continuous carbon structure. However, because of the random orientation of the platelets, microvoids can form as pathways for water or hydrogen permeation necessitating a minimum carbon layer thickness. That is, the carbon layer thickness required to insure hermeticity depends on the carbon structure. Generally speaking, it is preferable to have a high graphite content with the corresponding large crystal size with the platelets aligned to the surface of the fiber. Because the alignment of the platelets indicates the continuity of the carbon layer, the issue of carbon layer roughness has been explored. For example, Aikawa, et. al., analyzed car-

bon-coated fibers with similar carbon thicknesses, but with increasing roughness as measured by AFM. The samples with a smoother surface exhibited lower hydrogen-induced loss; the authors concluded that a smaller boundary area reduces the pathways for hydrogen diffusion.<sup>12</sup> In another study, roughness measured on STM was further related to resultant fiber strength.<sup>13</sup>

The strength penalty associated with carbon-coated fibers as compared to untreated fibers is well documented. The reasons for the strength reduction with carbon are related in part to the deposition method used and in part with the carbon layer itself. The thermal decomposition of the hydrocarbon gas generates soot particles as a side-product which can reduce fiber strength and interfere with the chemical bonding on the glass surface. If the reactor is hot enough, spontaneous reaction of the hydrocarbon may occur leading to soot in the reactive gas and deposited to the inside of the reactor. Therefore it is necessary to control the reactor design and deposition process to minimize soot generation and interaction with the bare fiber. The carbon layer itself is as brittle as the glass and, because it is deposited at an elevated temperature and has a different coefficient of thermal expansion than glass, will apply a residual tensile stress to the fiber upon cooling. In addition, because the carbon layer has a lower failure strain than pristine silica, the carbon layer will fail before the fiber. Several studies have indicated that a thicker carbon layer will produce a lower fiber strength but an improved resistance to fatigue and hydrogen ingress.<sup>14</sup> For applications where a fiber will be cabled and operated below the fiber proof test level, a thicker carbon layer may be preferable to ensure a min-

imum thickness is present to exclude diffusion pathways caused by microvoids. Glaesemann has concluded that a carbon-coated fiber with a high fatigue constant ( $>150$ ) can operate at up to 80% of the proof test level as opposed to silica fiber (with an "n" value around 20) that should not operate with a long-term stress above 20-30% the proof test level.<sup>15</sup> In addition, for fibers used in harsh environments where static fatigue may be accelerated through water or OH<sup>-</sup> permeation, DiMarcello, et. al., have concluded that an optical fiber should have a tensile strength of 500 kpsi or greater and a minimum fatigue factor of 150.<sup>16</sup>

Based upon this body of information, we here present our efforts to extend and improve the hermetic carbon deposition process within the confines of the low-speed draw process.

## DATA AND DISCUSSION

### Carbon deposition process

Fiber samples were drawn to a 125 $\mu$ m glass diameter and coated with a carbon layer then a thermally-cured polyimide coating to a size of 130 $\mu$ m. The electrical resistance of the carbon layer was measured with an ohm-meter after the draw speed had stabilized and before the polyimide coating was applied. By controlling the final draw speed, the pyrolysis temperature of the precursor hydrocarbon gases at the reactor was held close to a standard for each test. Two hydrocarbon precursor gases were used and two mixtures of gases in different concentrations: hydrocarbon "B" (OFS's current standard or "base" hydrocarbon), hydrocarbon "A" (designated as "additive"), an 8:1 mixture of

B:A by volume, and a 2:1 mixture of B:A by volume. To isolate the test fiber, short lengths were drawn to avoid deposition fluctuations caused by draw speed changes. The electrical resistance of the fiber was rechecked after drawing by stripping off the polyimide coating and measuring at varying points and lengths along the fiber.

To determine the effect of the different gas treatments on the applied carbon layer, samples were tested with Raman spectroscopy at Sandia National Laboratories. The samples were excited at a 514nm wavelength and the relative intensities of the Raman shift were measured. Pyrolytic graphite shows strong characteristic peaks at  $\approx 1360$   $\text{cm}^{-1}$  and  $\approx 1580$   $\text{cm}^{-1}$  which are referred to as the "D" and "G" peaks, respectfully denoting the graphite disorder induced mode and the graphite E<sub>2g</sub><sup>2</sup> modes in the carbon structure.<sup>17</sup> Because the Raman shift is expressed as a relative intensity, the ratio of the "D" to the "G" peaks is often used to compare carbon phase structures. As Figure 1 indicates, the symmetries between the Raman curves and a comparison of the G/D ratios suggest the carbon structures of the different samples are very similar.

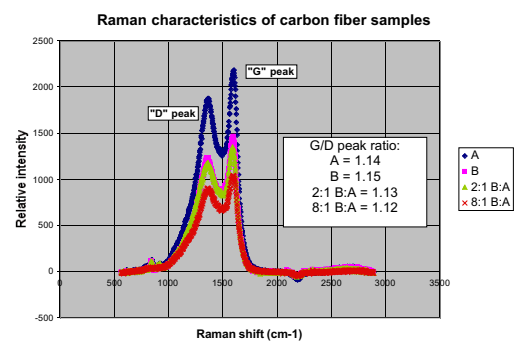


Figure 1

Since the pyrolytic carbon composition is similar from sample to sample, we can infer that the carbon layer resistance is near-equal when used in the layer thickness equation. Based on previous Spectran research<sup>18</sup>, we use the 16 kΩ-cm resistance / 300Å carbon thickness as a basis for comparison to test fibers. Thus, using the equation above, the carbon layer thicknesses were calculated:

Table 2: Estimated carbon layer thickness

	Average Resistance	Estimated Thickness
Hydrocarbon "B"	16.0 kΩ/cm	300Å
Hydrocarbon "A"	45.5 kΩ/cm	105Å
8:1 B:A mix	11.4 kΩ/cm	424Å
2:1 B:A mix	5.9 kΩ/cm	812Å

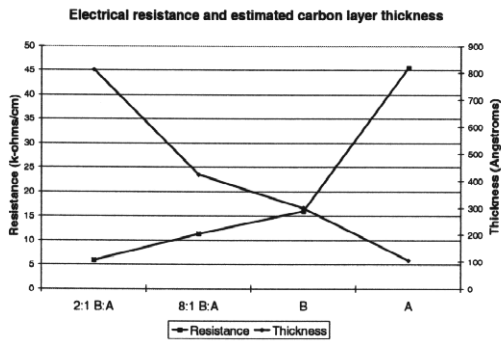


Figure 2

The addition of hydrocarbon "A" to the standard "B" has a marked effect on the carbon deposition process. This may be explained in part due to the fact that "A" is exothermic upon decomposition. It is proposed that the exothermic decomposition of hydrocarbon "A" enhances the cracking of the "base" hydrocarbon "B". Thus, an 12.5% addition of "A" leads to

a 41% carbon layer thickness increase for an 8:1 mixture as measured by electrical resistance. The 2:1 mixture (50% addition of "A") yields a thickness increase of 270%. The addition of the exothermic hydrocarbon is critical for the low-speed draw process since the reaction zone is usually much smaller than for a high speed process. By mixing the hydrocarbon gases, the reaction zone for decomposition is extended and a thicker carbon layer can be deposited.

It should be noted that when hydrocarbon "A" is used by itself in a low-speed draw run, the deposition process appears to be hindered by the inordinate amount of soot generated. During test runs, soot emerging from the reactor had to be directed from the fiber and there were difficulties tuning in the deposition process. The soot generated using this particular hydrocarbon precursor alone would clearly impart a detrimental effect on the fiber strength. The resulting carbon layer was calculated at only 105Å and appeared much lighter in appearance than the standard fiber.

### Fiber strength

Fiber strength was determined by performing two-point bend tests; 40 samples of each fiber were tested at a 4%/minute strain rate. A fiber sample without carbon was also tested to determine the strength penalty associated with the low-speed carbon deposition process.

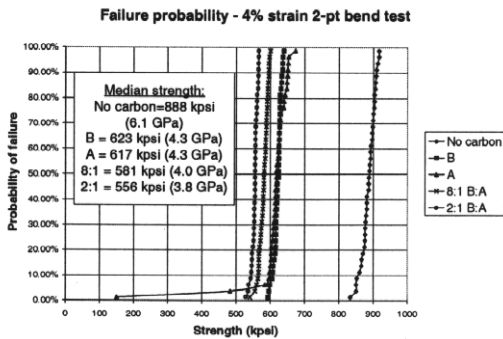


Figure 3

Although the data indicates a tight distribution, the strength penalty associated with carbon is >250 kpsi (1.7 GPa). Tensile strength tests (4%/min strain) comparing the standard carbon fiber ("B") with a polyimide coating to polyimide fiber without carbon indicates a median strength drop of ≈170 kpsi (1.2 GPa); a similar shift is apparent in the dynamic fatigue test data shown below (figure 5). In addition, although hydrocarbon "A" exhibits a high intrinsic strength associated with the bonding of the carbon to the glass fiber surface, the soot generated during the deposition process likely caused the two low-strength measurements that dramatically altered the calculated Weibull slope (figure 4).

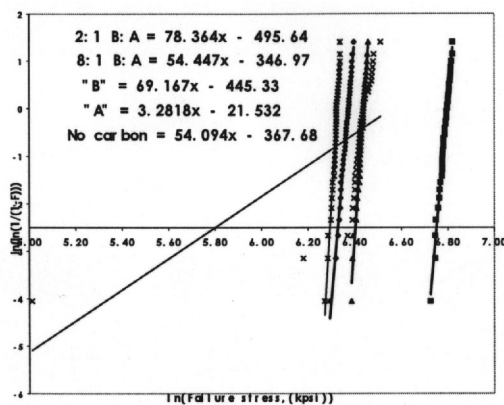


Figure 4: Weibull distribution

## Dynamic fatigue

To gauge the effect of carbon on the dynamic fatigue characteristics of the fiber, fibers were strained at different rates to determine dynamic strength and fatigue parameters as dictated under FOTP-28. In this test, 125µm/155µm glass/polyimide fiber samples were strained at 25%/min, 2.5%/min, 0.25%/min and 0.025%/min; the resulting break stresses were used to calculate the stress corrosion factor (n). The samples tested were two non-carbon and two carbon-coated fibers, the latter using the standard "base" hydrocarbon.

Table 3: Fatigue parameters for test fibers

	$n_d$
Carbon "B"/polyimide sample #1	206
Carbon "B"/polyimide sample #2	205
No Carbon/polyimide sample #1	22
No Carbon/polyimide sample #1	21

Considering that the samples were produced from different runs, there is good agreement both in terms of median strengths and calculated fatigue parameters suggesting a stable process.

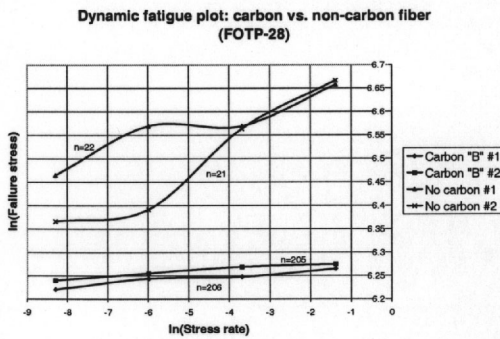


Figure 5

Samples of the test carbon fibers were strained at 25%, 2.5%, and .25%/min using two-point bend testing. Twenty samples were broken at each strain rate along with a non-carbon fiber sample. As with the standard FOTP procedure, the dynamic fatigue parameter was calculated based on the slope of the failure strength/strain rate slope. The stress corrosion factor as calculated were as follows:

Table 4: Fatigue parameters from 2-pt. bend test

	$n_d$ (2-point)
Carbon "B"	> 300
Carbon "A"	25
Carbon 8:1 B:A	> 300
Carbon 2:1 B:A	> 300
No Carbon	17

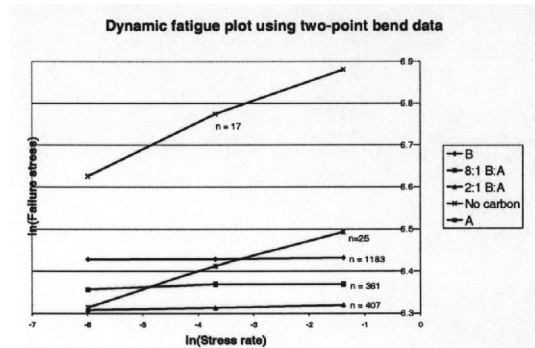


Figure 6

As with the fiber strength data, it is evident that the non-carbon fiber has a higher overall strength. However, the dynamic fatigue factor is an order of magnitude lower than the carbon-coated samples which show little degradation in strength at lower strain rates. The exception for hydrocarbon "A" is also consistent with the strength data. Since the "A" carbon is very thin, it provides minimum protection from fatigue. Thus, the slope for the "A" carbon fiber is similar to the fiber with no carbon coating.

### Carbon layer effect on strength

The carbon fiber samples were analyzed by atomic force microscopy (AFM) at Sandia National Laboratories. The mean roughness was calculated from measurements in a discrete area of 4mm<sup>2</sup> or below to minimize variability caused by the curvature of the fiber and isolate the coating from extraneous contamination on the carbon surface. The mean roughness are noted here along with the estimated carbon layer thickness:

Table 5: Carbon roughness and thickness data

	Roughness	Thickness
Carbon "B"	16.6Å	300Å
Carbon "A"	15.8Å	105Å
Carbon "8:1"	38.7Å	424Å
Carbon "2:1"	24.6Å	812Å

As the data suggests, the roughness of the carbon surface does not appear to be directly related to the thickness of the applied layer. However, while a heterogeneous mixture of hydrocarbon gases may lead to an overall thicker applied layer, it may be postulated that a rougher morphology is based on the different reactions of the precursor hydrocarbons. That is, carbon platelets of a varied size are evolving at different temperatures both as a result of the mixed hydrocarbons and of the extended reaction zone.

The effect of carbon layer roughness and thickness on fiber strength may be seen here in Figures 7 and 8:

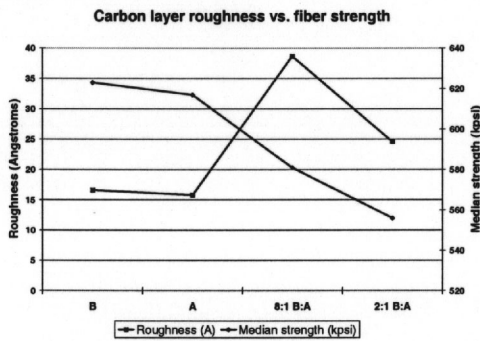


Figure 7

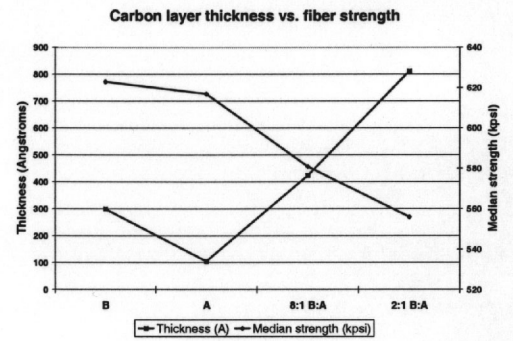


Figure 8

While there is some correlation with fiber strength versus carbon roughness, a stronger correlation of coating thickness is apparent. As noted, this may be attributed to the presence of pre-reacted carbon soot impacting the fiber during the deposition process. The "A" hydrocarbon alone was very sooty and the increasing concentration ratio may indicate the addition of the exothermic gas will lead to lower strength because of soot. The symmetry of the thickness trend to the median strength makes a strong case for thickness as the determinant of overall fiber strength. As noted, the thicker layer may be more susceptible to cracking due to the added residual stress on the carbon layer. In addition, if the deposited platelets are of varying sizes and phases, the alignment and bonding of the disparate platelets may lead to a weaker carbon layer due to additional microvoids in the structure.

## CONCLUSIONS

In our efforts to improve and extend the low-speed carbon deposition process, we have shown the pyrolysis of a precursor hydrocarbon gas can be augmented with the addition of a hydrocarbon gas that is exothermic upon decomposition. The gas mixture produces a carbon layer with an

increased surface roughness, but a deposited layer that is significantly thicker than when using a single precursor gas. The thicker carbon layer results in a fiber strength penalty, but has no appreciable effect on the stress corrosion factor when calculated using two-point bend testing. Based on the thickness data (as measured by electrical resistance), the strength and dynamic fatigue data of the test fibers, it is theorized the carbon layers deposited using the gas mixture will provide better protection from water and hydrogen ingress than the current base standard. Work to show the effect of the new carbon layer on water and hydrogen ingress is in progress.

## **ACKNOWLEDGMENTS**

The authors would like to thank Brian E. Slyman for support in generating fiber samples, Vessela Krasteva for performing dynamic fatigue tests and Jim Krumhansl of Sandia National Laboratories for arranging testing. Sandia is a multiprogram laboratory operated by Sandia Corporation, a Lockheed Martin Company, for the United States Department of Energy under Contract DE-AC04-94AL85000.



Eric A. Lindholm received his B.S. degree in Ceramic Engineering and his B.A. degree in English from Rutgers University in 1991. While at Rutgers, he worked in the Fiber Optics Materials Research Program under Dr. George Sigel. After college, he spent five years at Spectran Communication Fiber Technologies as a Fiber Draw Engineer before moving to Spectran Specialty Optics Company in 1996, which was later purchased by OFS. As Senior Product Development Engineer at OFS, Specialty Photonics Division, he has focused much of his efforts on the development of optical fiber for adverse environment applications.

## REFERENCES

---

- <sup>1</sup> Kurkjian, C.R., Simpkins, P.G., Inniss, D., "Strength, Degredation, and Coating of Silica Lightguides", Journal of the American Ceramic Society, May 1993.
- <sup>2</sup> Biswas, D.R., Kurkjian, C.R., Yuce, H.H., "Hermetic Coatings for Optical Glass Fibers", International Wire and Cable Symposium, 1995.
- <sup>3</sup> Ibid.
- <sup>4</sup> "Optical Fiber Telecommunications II" Miller & Kaminow, eds, p. 153, 1988.
- <sup>5</sup> Dimarcello, F.V., et. al. "High speed manufacturing process for hermetic carbon coated optical fibers", Optical Fiber Communications Conference, 1990.
- <sup>6</sup> Ibid.
- <sup>7</sup> Huff, R.G., Dimarcello, F.V., Hart, Jr. A.C., Walker, K.L., "Deposition of Hermetic Coatings on Silica Fibers" Materials Research Society Symposium, 1990.
- <sup>8</sup> Tuzzolo, M.R., Allegretto, A.E., Urruti, E.H., "Hermetic Product Performance: Ensuring the Uniformity of the Carbon Layer", International Wire & Cable Symposium, 1993.
- <sup>9</sup> Nakamura, et. al., "Structures and Characteristics of Carbon Films on Optical Fibers", International Wire & Cable Symposium, 1994.
- <sup>10</sup> Sikora, et. al., "Examination of the Strength Characteristics, Hydrogen Permeation, and Electrical Resistivity of the Carbon Coating of a Number of 'Hermetic' Optical Fibers", International Wire & Cable Symposium, 1991.
- <sup>11</sup> Cusanello, V.A., Jacobson, N.J., Supczak, M.J., Stupak, P.R., "A Hermetic Carbon/Polyimide Coating Combination for Adverse Environments", International Wire & Cable Symposium, 1995.
- <sup>12</sup> Aikawa, et. al., "Characteristics of Carbon-Coated Optical Fibers and Structural Analysis of the Carbon Film", International Wire & Cable Symposium, 1993.
- <sup>13</sup> Yoshizawa, N., Katsuyama, Y., "High-strength Carbon-coated Fiber", Electronics Letters Vol. 25, 1989.
- <sup>14</sup> Moore, K., Dwivedi, A., Sikora, E., "Review of Characteristics and Applications of Commercially Available Carbon-Coated Hermetic Fiber", International Wire & Cable Symposium, 1995.
- <sup>15</sup> Glaesemann, G.S., Gulati, S.T., "Design Methodology for the Mechanical Reliability of Optical Fiber", Optical Engineering 30(6), 709-715, 1991.
- <sup>16</sup> DiMarcello, et. al., U.S. Patent #5,000,541, 1991.
- <sup>17</sup> Dennison, J.R., Holtz, M., Swain, G., "Raman Spectroscopy of Carbon Materials", Spectroscopy 11(8), Oct. 1996.
- <sup>18</sup> Cusanello, V.A., Jacobson, N.J., Supczak, M.J., Stupak, P.R., "A Hermetic Carbon/Polyimide Coating Combination for Adverse Environments", International Wire & Cable Symposium, 1995.

---

### NOTE:

*All rights to this publication and the intellectual property herein have been transferred from the original owner, SpecTran, to OFS.*



Leading Optical Innovations

SPECIALTY PHOTONICS DIVISION



*Leading Optical Innovations*

*SPECIALTY PHOTONICS DIVISION*

SPD-WP02-0103